Ultrafast optical control of electron spin coherence in charged GaAs quantum dots

M. V. Gurudev Dutt,[1,*] Jun Cheng,[1] Yanwen Wu,[1] Xiaodong Xu,[1] D. G. Steel,[1,†] A. S. Bracker,[2] D. Gammon,[2] Sophia E. Economou,[3] Ren-Bao Liu,[3] and L. J. Sham[3]

[1]*The H. M. Randall Laboratory of Physics, The University of Michigan, Ann Arbor, Michigan 48109, USA*

[2]*The Naval Research Laboratory, Washington D.C. 20375, USA*

[3]*Department of Physics, The University of California-San Diego, La Jolla, California 92093, USA*

(Received 9 February 2006; revised manuscript received 28 June 2006; published 13 September 2006)

Impulsive stimulated Raman excitation with coherent optical fields is used for controlling the electron spin coherence in a charged GaAs quantum dot ensemble through an intermediate charged exciton (trion) state. The interference between two stimulated Raman two-photon quantum mechanical pathways leading to the spin coherence allows us to control the electron spin coherence on the time scale of the Larmor precession frequency. We also demonstrate, both theoretically and experimentally, that ultrafast manipulation of the spin coherence is possible on the time scale of the optical laser frequency, and analyze the limitations due to the trion and spin decoherence times.

DOI: 10.1103/PhysRevB.74.125306 PACS number(s): 78.67.Hc, 78.30.Fs, 78.47.+p, 42.50.Md

I. INTRODUCTION

A unique feature of quantum mechanics is the ability for a system to exist in coherent superpositions of the stationary quantum states. Long-lived quantum coherences are responsible for a remarkable variety of phenomena in quantum optics with atomic ensembles such as electromagnetically induced transparency (EIT), coherent population trapping in dark states, storage, and retrieval of nonclassical states of light, and nonlinear optics at the single photon level.[1,2] Quantum coherence also forms the basis for the massive parallelism leading to exponential speedup in quantum algorithms relative to classical algorithms. Because of its anticipated long decoherence time ($T_2 \sim 50\ \mu$s),[3] required for quantum error correction,[4] the spin vector of an electron in a charged quantum dot (QD) has been proposed as a qubit for quantum computing (QC).[4–6] Long spin relaxation times ($T_1 \sim 1-20$ ms) (Refs. 7–9) and spin dephasing times ($T_2^* \sim 10$ ns) (Refs. 10–12) have already been measured. Charged QDs thus represent a possible route towards engineered solid-state implementations of ion-trap physics, which have proven to be extremely successful in demonstrating basic quantum logic operations.[13,14] Optical control of long-lived spin coherence is an enabling step for advances in both the fields of quantum information processing[6,15–17] and semiconductor device research based on EIT.[18]

Coherent optical control through the interference between quantum-mechanical pathways created by a series of phase-locked optical pulses is a well-established technique in atoms and molecules.[19–22] In solids, the challenge of the short decoherence time of the elementary optical excitations has been overcome by lowering the dimensionality in quantum well (QW) and QD heterostructures. Coherent optical control of the population,[23] orientation,[24] and transverse spin polarization[25] of QW excitons, as well as QD exciton wave function engineering[26] has already been achieved. Recently, it has been shown that quantum interference between one- and two-photon processes can be used to control macroscopic charge and spin currents in bulk semiconductors as well.[27,28] While such experiments directly manipulate the elementary excitations created by optical injection of electron-hole pairs in the semiconductor nanostructure, the relatively short decoherence times [0.1–1 ns in QDs (Refs. 29 and 30)] remains a critical challenge for QC.

In this work, we report on the coherent optical control of electron spin coherence, on a pico- and femto-second time scale, in the ground state of negatively charged GaAs QDs. Ultrafast coherent optical control based on impulsive stimulated Raman excitation is used for controlling the electron spin coherence in a charged GaAs quantum dot ensemble through an intermediate charged exciton (trion) state. The addition of excitations from different stimulated Raman two-photon quantum mechanical pathways leads to constructive or destructive interference of the net ensemble spin coherence, and allows us to control the electron spin coherence on the time scale of the Larmor precession. Interestingly, we also show that ultrafast manipulation of the spin coherence is possible on the time scale of the inverse laser frequency. We analyze the limitations due to the trion and spin decoherence times. The results indicate that not only can a long-lived spin coherence be induced between two orthogonal electron spin states, but also that this coherence accurately preserves the relative phase on the time scale of the spin decoherence time, allowing for the potential to perform multiple state rotations and spin switching.

II. THEORY

When there is no magnetic field present, the QD conduction band ground state sublevels, distinguished by the electron spin direction, are degenerate in accord with Kramer's theorem. Absorption of a photon leads to a trion state that is composed of a singlet pair of electrons bound to a heavy hole whose spin can point up or down along the growth axis, designated as the z axis. When a magnetic field perpendicular to the z axis (the Voigt geometry) is applied, the singlet state of electrons remains unaffected and the heavy-hole spin remains pinned to the growth axis due to the strong spin-

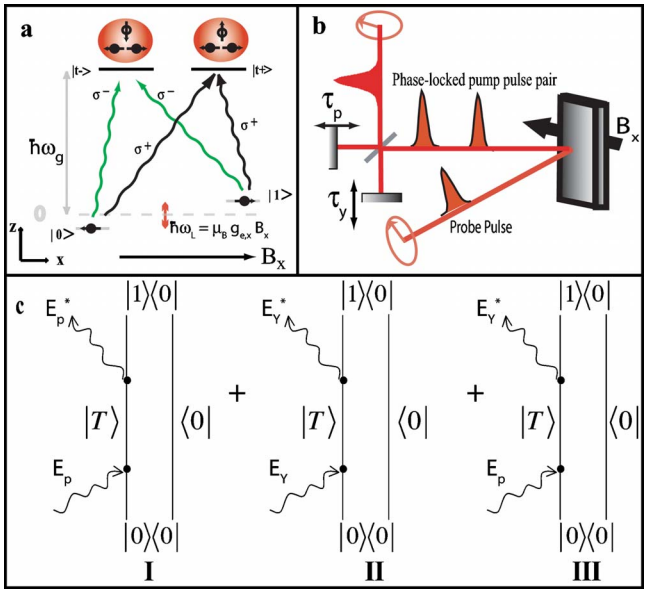

FIG. 1. (Color online) (a) Excitation picture for the charged QD, with ground states $|g=0,1\rangle$ denoting electron spin projections $|\pm\frac{1}{2}\rangle$ along the x-axis symmetrically split by $\hbar\omega_L=\mu_B g_{e,x}B_x$, where μ_B is the Bohr magneton. The degenerate trion states $|t\pm\rangle$ are labeled by the heavy-hole angular momentum projection $|\pm\frac{3}{2}\rangle$ along the growth (z) axis, with transition energy $\hbar\left(\omega_g\pm\frac{\omega_L}{2}\right)$. Solid (gray) lines denote transitions excited by $\sigma^+(\sigma^-)$ light. (b) Schematic diagram of the experimental setup. (c) Double-sided Feynman diagrams for different quantum-mechanical pathways due to SR2Ps leading to creation of spin coherence. $|T\rangle$ is used to denote either trion state $|t\pm\rangle$. There is a corresponding set of diagrams (not shown) starting from the density operator $|1\rangle\langle 1|$.

orbit interaction and quantum confinement. This leads to the energy level diagram shown in Fig. 1(a), with upper levels remaining degenerate, and lower levels split by the Zeeman energy of the electron.[6] While the details of the polarization dependence of the signal can be correctly accounted for only by this four level scheme, the essential features of our experiment can be understood by considering a three-level Λ system, similar to those employed in demonstrations of EIT. Figure 1(b) shows a schematic diagram of the experimental setup, with a Michelson interferometer used to generate phase-locked primary ($\mathbf{E}_p$) and control ($\mathbf{E}_y$) laser pulses. The delay between the primary and control pulses is controlled by a mechanical delay line (τ_y) and a piezoelectric transducer (τ_p). A simple view of coherent control is based on the understanding that each laser pulse, through the stimulated Raman two-photon process (SR2P), creates a coherent superposition of the spin states.

If the initial state of the electron is described by a pure state, $|0\rangle$ say, the ideal spin state produced after the excitation pulses is given, to second order in perturbation by the applied optical fields, by $\sqrt{1-\alpha_p-\alpha_y}|0\rangle+\sqrt{\alpha_p}e^{-i\omega_L(t-\tau_x)}|1\rangle+\sqrt{\alpha_y}e^{-i\omega_L(t-\tau_y)}|1\rangle$. Here α_j $(j=p,y)$ is the probability of excitation in a given SR2P with $\alpha_j\propto I_j$, where I_j is the peak intensity of the corresponding jth pulse, and ω_L is the Larmor frequency. In our measurements, we need to average both over the repetitions of pulse sequences and over the dot ensemble. Both averages of a state may be represented by a density matrix.[1] At the high temperatures of our experiment relative to the Zeeman splitting of the ground state, the initial spin state is unpolarized with its density matrix taken to be $1/2(|0\rangle\langle 0|+|1\rangle\langle 1|)$. The second order state has the spin coherence $e^{-i\omega_L(t-\tau_y)}(\sqrt{\alpha_y}+\sqrt{\alpha_p}e^{-i\omega_L(\tau_y-\tau_p)})|1\rangle\langle 0|$, which survives the averaging with a decaying factor that will be shown later. The two contributions to the coherent superposition can now add constructively or destructively depending on the phase difference, giving rise to interference.

The double-sided Feynman diagrams for the SR2Ps, representing the time evolution of some of the density matrix elements,[31] are shown in Fig. 1(c). Each Feynman diagram gives a contribution to the spin coherence, where the individual photons at times τ_i, τ_j $(i,j=y,p)$ in the process satisfy the two-photon resonance condition $\Delta_i-\Delta_j=\pm\omega_L$ with $\Delta_{i,j}=\omega_{i,j}-\omega_g$ being the detuning from the optical resonant frequency. Interference between the diagrams will occur only when the spin coherence $\rho_{1,0}$ is nonvanishing. In addition, the intermediate state in all three diagrams is seen to be the trion coherence $\rho_{T,0}$, requiring the second photon to arrive before both the trion and spin coherence vanish. In the process for the control of coherence evolution depicted by diagrams I and II, since the second photon is from the same laser field, the requirement is T_2, $T_2^{\text{trion}}>\tau$, where T_2 (T_2^{trion}) is the decay time of the spin (trion) coherence, and τ is the pulse-width. In diagram III, the requirement is T_2, $T_2^{\text{trion}}>\tau_j-\tau_i$.

A systematic description with all three incident pulses can be obtained using the Feynman diagrams in Fig. 1(c) to solve the density matrix master equation [Eq. (1)], in the limit of δ-function pulses, for the four-level system shown in Fig. 1(a)

$$\frac{d\rho}{dt}=\frac{1}{i\hbar}[H,\rho]+\left.\frac{\partial\rho}{\partial t}\right|_{\text{relaxation}}. \tag{1}$$

For example, in diagram III, the primary pulse coherently excites the trion coherence $\rho_{T,0}$, which is converted by the control pulse into the spin coherence $\rho_{1,0}$. The probe pulse measures the state of the spin superposition, by converting it into a nonlinear polarization ($\propto\rho_{T,0}$) that copropagates with the probe field. The perturbation sequence is shown below

$$\rho_{0,0}\xrightarrow{E_P(\sigma^-)}\rho_{t-,0}\xrightarrow{E_Y^*(\sigma^-)}\rho_{1,0}\xrightarrow{E_X(\sigma^\mp)}\begin{cases}\rho_{t+,0}\\ \rho_{t-,0}\end{cases}.$$

In addition, there exist several other pathways which involve population of the excited trion state, but for probe delays long compared to $T_1^{\text{trion}}\sim 50$ ps (Refs. 11 and 32) the signal will be dominated purely by the oscillating spin coherence. The effective Rabi frequency of the pulse is estimated from the formula $\Omega_{\text{eff}}=\sqrt{\Omega_i^2+\Omega_j^2}$, $(i,j=y,p)$[1,2] where $\Omega_i=\frac{\mu E_i(\omega_i)}{\sqrt{2}\hbar}$, μ is the dipole moment, and $E_i(\omega_i)$ is the peak electric field at the frequency ω_i in the Raman process. Assuming $\mu=40$ Debye,[33] $E=6.3\times10^4$ V/m (see below), we estimate that the pulse area is $\sim\pi/8$.

We showed elsewhere[11] that the spin coherence $\rho_{1,0}$ (off-diagonal components of ρ_{spin}) created through impulsive stimulated Raman excitation can be probed by the polarization dependent differential transmission (DT) signal. The spin coherence obtained for a homogeneously broadened system with both primary and control fields incident, due to the interference between the diagrams shown in Fig. 1(c), is found to be

$$\mathrm{DT}_{\mathrm{diff}} \propto \underbrace{I_p \cos(\omega_L \tau_{xp}) e^{-\tau_{xp}/T_2}}_{I} + \underbrace{I_y \cos(\omega_L \tau_{xy}) e^{-\tau_{xy}/T_2}}_{II} + \underbrace{2\sqrt{I_p I_y} e^{-\tau_{xy}/T_2} e^{-\tau_{yp}/T_2^{trion}} \cos(\omega_g \tau_{yp}) \cos\left(\omega_L \tau_{xy} - \frac{\omega_L \tau_{yp}}{2}\right)}_{III}, \tag{2}$$

where $\tau_{ij}=\tau_i-\tau_j$ for $i,j=x,y,p$, I_j is the peak intensity, and $\mathrm{DT}_{\mathrm{diff}}$ is the difference in DT signals for parallel and orthogonal circular polarizations of the pump and probe fields. Each term in Eq. (2) corresponds to a SR2P depicted in Fig. 1(c) that produces spin coherence from the initial unpolarized spin ensemble, which can interfere with the other diagrams provided the induced coherence does not vanish, even though the individual primary and control pulses may have zero overlap. Impulsive SR2Ps have been used extensively to control the coherent vibrational modes of molecules[34,35] and solids,[36] and more recently to generate entangled states of donor-bound electron spins in QWs.[37] Spontaneous emission generated coherence,[11,38] which has been neglected as being noncentral to our discussion here, was also included in a more complete calculation, and found only to change the overall phase and amplitude of the results. The absence of the detuning from the trion state Δ in Eq. (2) is due to the assumption of δ-function pulses. In the presence of inhomogeneous broadening of the Zeeman levels, averaging of Eq. (2) leads to an effective spin dephasing time $T_2^* \leq T_2$. Previous measurements suggest that in these QDs, $T_2^{\mathrm{trion}} \sim 50$ ps,[37,38] and $T_2^* \sim 10$ ns,[10,11] while T_2^* at the finite field used for this experiment is 750 ps. For the case where the finite bandwidth of the pulses becomes important, a full calculation taking the spectrum of the pulses into account is required.

III. EXPERIMENTAL RESULTS AND DISCUSSION

In our experiments, the sample consisted of interface fluctuation GaAs QDs, formed by growth interrupts at the interface of a narrow (4.2 nm) GaAs QW, which were remotely doped with electrons.[39] The etched sample was mounted in a superconducting magnetic cryostat held at 4.8 K, with the magnetic field fixed at $B_x=2.2$ T. The optical pulses were obtained from a mode-locked Ti:Sapphire laser (repetition rate 76 MHz) with a shaped pulse bandwidth (FWHM $=0.35$ meV, $\tau \sim 5.4$ ps) that exceeds the splitting between the electron spin states. The pump fields (primary and control) are circularly polarized, while the probe field is linearly polarized, and all are degenerate and resonant with the trion state. The repetition period of the laser is longer than the decay time for the spin polarization, which is limited by $T_2^* \sim 750$ ps at $B_x=2.2$ T, thereby ensuring that each set of pulses acts on the same quantum state. We verified that the nonlinear response was within the $\chi^{(3)}$ regime for the primary and control peak intensity of 2.7 kW/cm.[2]

After the sample, a quarter-wave plate and polarizing beam splitter are used to direct the parallel and orthogonal circularly polarized components (relative to the pump fields) of the probe beam to two balanced photodiodes, whose difference signal is input to a lock-in amplifier. The pump fields are spatially separated from the detectors through a small angle. Both pump and probe fields are modulated ~ 1 MHz, and the difference frequency is input as the reference to the lock-in amplifier. The signal in the lock-in amplifier is proportional to the difference in DT response for configurations where the pump and probe fields have parallel or orthogonal circular polarizations. The classical auto-correlation signal is obtained by removing the sample, and letting both pump fields fall on the photodiode. Varying the delay between the fields now corresponds to measuring the (classical) coherence time of the laser pulses. From first-order coherence theory, the Fourier transform of this auto-correlation function gives the spectrum of the pulse, used to deconvolve the signal in Fig. 4.

Figure 2 shows the spin coherence obtained as a function of both delays (τ_x, τ_y), with resonant excitation via the trion state displayed in Fig. 3(a) [showing the nonlinear optical spectrum of both the trion (T) and exciton (X)].[11,39] Each point on the surface represents the average of $\sim 10^7$ shots for a given set of delay parameters. The peak at $\tau_x=0$ ps in Fig. 2 represents the arrival time (τ_p) of the primary pulse, which is fixed during this experiment. The arrival of the control pulse is also visible as a second peak, with the arrival time τ_y varying over a full Larmor precession period $\tau_L=2\pi/\omega_L$ $=260$ ps of the oscillation, A horizontal slice through the data in Fig. 2, at $\tau_y=120$ (240) ps, is shown in Figs. 3(b) and 3(c), demonstrating destructive (constructive) interference in the spin coherence. The data in Fig. 3(c) at $\tau_y=240$ ps (dashed line), showing constructive interference in the spin coherence, is contrasted with the data with only the primary pulse (dotted line), where the shaded area marks the differ-

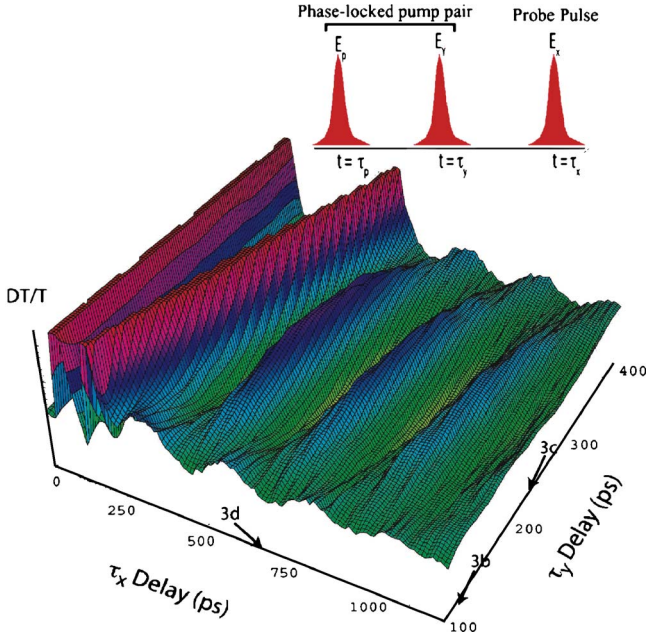

FIG. 2. (Color online) Coherent optical manipulation of electron spin coherence in charged quantum dots. The data shown is the DT signal as a function of (τ_x, τ_y), with the magnetic field B_x=2.2 T. The peaks show the arrival of the primary and control pulses. The spin coherence is read out by the probe, with the probe delay scanned along the τ_x-axis, while the τ_y-axis denotes the delay between the control and primary pulses. Inset shows the temporal sequence of laser pulses for coherent optical control of the spin coherence. The arrows represent the position where the delay of the corresponding laser pulse is parked for the experiments of Fig. 3.

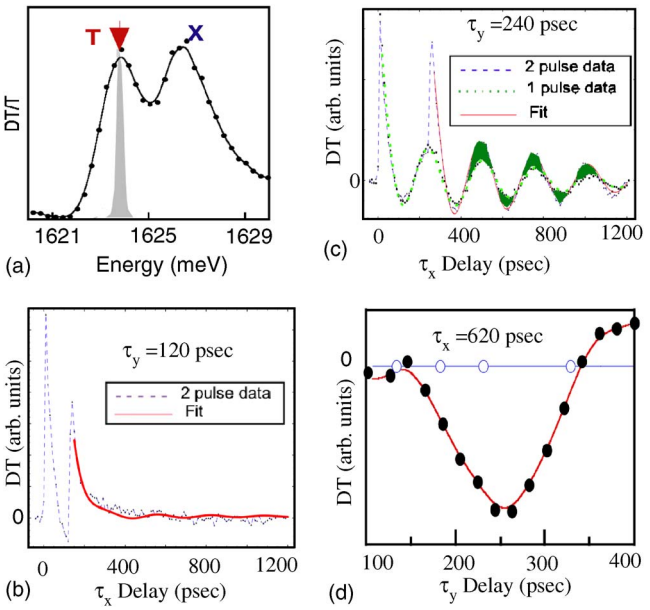

FIG. 3. (Color online) (a) DT spectrum (no control pulse) with the pump-probe delay fixed at +10 ps. The shaded region is the pulse spectrum with the pump spectral position, fixed for all the other experiments denoted by the red arrow, and T (X) labels the trion (exciton) resonances. (b), (c) Horizontal slice from Fig. 2 at τ_y=120, 240 ps, respectively, with dashed lines representing data, and solid lines representing fits to the data using Eq. (2). In (c) dotted lines represent the fit to the single pump pulse data. The shaded area represents the difference in signals obtained with and without the control pulse. (d) Vertical slice (solid circles) from Fig. 2 at τ_x=620 ps. Open circles are data from a classical first-order auto-correlation between the primary and control fields.

ence. A vertical slice through the data in Fig. 2 at τ_x =620 ps is shown in Fig. 3(d), illustrating the interference as τ_y is varied (solid circles). The open circles are obtained from a classical first-order autocorrelation between the primary and control fields. The classical autocorrelation vanishes and is not dependent on τ_y, signifying that the variation in the signal is not due to classical interference between the pulses. As the ratio τ_y/τ_L varies from 0.5 to 1, we note that the beat amplitude goes from 0 to its maximum value.

The analysis of the experimental data follows from Eq. (2). The third term in Eq. (2) becomes negligible for $\tau_{yp} \gg T_2^{\text{trion}} \sim 50$ ps, which is clearly satisfied in Fig. 2. At fixed probe delay τ_x, varying the control delay τ_y from $\tau_L/2$ to τ_L changes the argument of the cosine in term II from π to 2π, thereby causing destructive and constructive interference respectively. However, because of the finite T_2^* ($\sim$750 ps for B_x=2.2 T), the second term will decrease in magnitude, and therefore perfect contrast cannot be achieved. In fact, from the data in Fig. 3(c), we note that the enhancement factor observed experimentally for constructive interference is 1.8, in agreement with the theoretically expected value of 1.7. In both the Figs. 3(b) and 3(c), the solid lines denote fits to the data using the complete theory, including incoherent pathways, and using Eq. (2). The fits are obtained as follows: first the data with only one pump pulse is fitted (dotted lines) to the theory, and the same values are used in the fits shown in Figs. 3(b) and 3(c). The only free parameters are the amplitudes of the interfering terms. As in the other experimental demonstrations of coherent control in ensembles,[34,35,40,41] we note that we cannot distinguish between interference of two quantum pathways originating from single or multiple electron spins.

Ultrafast manipulation of the spin coherence is also possible experimentally using the dipole coherence of the trion transition. A quantum interferogram (QI) is taken at each different coarse delay τ_y, while varying τ_p on a subfemtosecond time scale using the piezo-electric transducer, and a sample scan is shown in the inset to Fig. 4 when τ_y=7 ps. Note that in the QI, the spin coherence is plotted, with the control-probe delay fixed at $\tau_x - \tau_y$=227 ps, well beyond the pulse overlap and the lifetime of the trion state. The measured signal is not sensitive to changes in the trion population, and hence the effect observed is entirely due to modulation of the spin coherence through the intermediate trion coherence. Each scan is fit to a cosine from which the amplitude is extracted, and denoted by the solid circles in the data of Fig. 4.

The femtosecond coherent control is made possible by the third path SR2P(III) shown in Fig. 1(c). Term III in Eq. (2) shows that the signal should exhibit ultrafast oscillations, at the optical transition frequency ω_g, as a function of the primary-control delay (τ_{yp}), and its envelope should decay exponentially with the dipole decoherence time T_2^{trion}. The

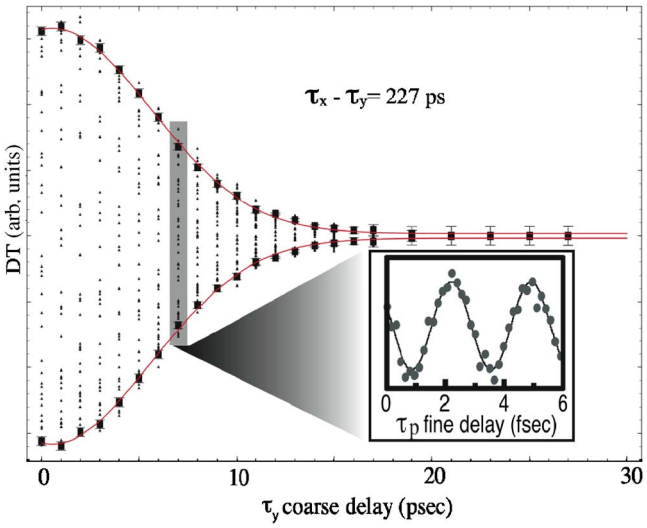

FIG. 4. (Color online) Femtosecond coherent optical control of spin coherence enabled through Feynman diagram III. Solid symbols denote data obtained by fixing the coarse delay τ_y, and scanning the fine delay τ_p. In theoretical calculations, the optical pulses are assumed Gaussian with the intensity given by $I(\omega)=\exp\left(-\frac{4\ln 2\omega^2}{\delta\omega^2}\right)$ ($\hbar\delta\omega=0.35$ meV), as measured by the classical interferogram.

control-probe delay τ_{xy} is fixed during the experiment, and the term $\omega_L\tau_{yp}/2$ varies negligibly on the experimental time scale $\tau_{yp}\ll 2\tau_L\sim 520$ ps. A similar effect was predicted for atomic states in Ref. 42, but the authors considered only population (rather than coherence) of the final state, and pulses that were off-resonant with the intermediate state, and thereby the control vanishes for non-zero pulse overlaps. In our case, the pulses are resonant with the trion state, and hence the control effect should be observed for a time comparable to the coherence time of the trion state. The ultrafast oscillations are observed in Fig. 4, but clearly the QI envelope does not follow an exponential decay.

The difference arises because of the finite pulse width, and the large inhomogeneous broadening in the optical transition frequency ω_g, which effectively reduces the decoherence time of the trion state. Assuming Gaussian functions for the inhomogeneous broadening and the optical pulse shapes, we carried out a finite pulse calculation for the femtosecond control, by assuming T_2, T_2^{trion}, $\tau_{xy}\gg\tau\sim 5.4$ ps, consistent with the experimental conditions. From the measured FWHM of the optical pulse intensity $\hbar\delta\omega=0.35$ meV, obtained by fitting the classical autocorrelation signal, we can deconvolve the classical signal to obtain T_2^{trion} and $\delta\omega_g$ where $\delta\omega_g$ is the FWHM of the inhomogeneous distribution in the trion transition frequency. The solid lines in Fig. 4 show the theoretical fit to the envelope data, yielding a trion decoherence time $T_2^{\text{trion}}=36\pm 1$ ps, in reasonable agreement with earlier measurements.[32,37] Since $\delta\omega<\delta\omega_g$ [see Fig. 3(a)], the decay of the QI envelope is mostly dominated by the laser pulse width, as shown in Fig. 4. The width of the inhomogeneous broadening can also be obtained, and was found to be $\hbar\delta\omega_g=0.7\pm 0.1$ meV, which is in good agreement with the data in Fig. 3(a).

In conclusion, the above measurements demonstrate coherent optical control of the spin polarization in charged QDs, both on the time scale of the Larmor precession period, limited by the decay of the spin coherence, and on a femtosecond time scale, limited by the decay of the trion optical dipole coherence. Coherent optical control, when extended to the regime of phase-locked laser pulses with sufficient intensity to perform π rotations, can be used for quantum state tomography, as has been shown in nuclear magnetic resonance experiments,[43,44] and for optical initialization and readout of the electron spin.[45] Such experiments will be necessary to understand the advantages and limitations of charged QDs in QC schemes, relative to the performance of existing ion-trap implementations. Experiments involving excited states have demonstrated that EIT can be observed with exciton spin coherence[46] or biexciton coherence[47] in QWs, but is limited by the short decoherence time. Recent measurements of ground state spin relaxation times in doped QWs, ranging from 200–2500 ps,[48,49] indicate that these effects could be substantially improved by using ground state coherences. As shown in this paper, the robustness of QD ground state spin coherence under optical manipulation makes it an attractive candidate for use in solid state optical switches and buffers based on EIT.[18]

ACKNOWLEDGMENTS

This work was supported in part by the U.S. ARO, NSA, ARDA, AFOSR, ONR, and the NSF.

*Present address: Department of Physics, Harvard University, 17 Oxford Street, Cambridge, MA 02138.
†Electronic address: dst@umich.edu

[1] M. O. Scully and M. S. Zubairy, *Quantum Optics* (Cambridge University Press, Cambridge, UK, 1997).
[2] M. D. Lukin, Rev. Mod. Phys. **75**, 457 (2003).
[3] I. Zutic, J. Fabian, and S. D. Das Sarma, Rev. Mod. Phys. **76**, 323 (2004).
[4] D. P. DiVincenzo, Fortschr. Phys. **48**, 771 (2000).
[5] D. Loss and D. P. DiVincenzo, Phys. Rev. A **57**, 120 (1998).
[6] A. Imamoglu, Fortschr. Phys. **48**, 987 (2000).
[7] A. Johnson, J. R. Petta, J. M. Taylor, A. Yacoby, M. D. Lukin, C. M. Marcus, M. P. Hanson, and A. C. Gossard, Nature (London) **435**, 925 (2005).
[8] M. Kroutvar, Y. Ducommun, D. Heiss, M. Bichler, D. Schuh, G. Abstreiter, and J. J. Finley, Nature (London) **432**, 81 (2004).
[9] J. M. Elzerman, R. Hanson, L. H. W. van Beveren, B. Witkamp, L. M. K. Vandersypen, and L. P. Kouwenhoven, Nature (London) **430**, 431 (2004).
[10] A. S. Bracker, E. A. Stinaff, D. Gammon, M. E. Ware, J. G. Tischler, A. Shabaev, Al. L. Efros, D. Park, D. Gershoni, V. L. Korenev, and I. A. Merkulov, Phys. Rev. Lett. **94**,

047402 (2005).
[11] M. V. G. Dutt, J. Cheng, B. Li, X. Xu, X. Li, P. R. Berman, D. G. Steel, A. S. Bracker, D. Gammon, S. E. Economou, R. Liu, and L. J. Sham, Phys. Rev. Lett. **94**, 227403 (2005).
[12] J. R. Petta, A. C. Johnson, J. M. Taylor, E. A. Laird, A. Yacoby, M. D. Lukin, C. M. Marcus, M. P. Hanson, and A. C. Gossard, Science **309**, 2180 (2005).
[13] F. Schmidt-Kaler, H. Hafner, M. Riebe, S. Gulde, G. P. T. Lancaster, T. Deuschle, C. Becher, C. F. Roos, J. Eschner, and R. Blatt, Nature (London) **422**, 408 (2003).
[14] D. Leibfried, B. DeMarco, V. Meyer, D. Lucas, M. Barrett, J. Britton, W. M. Itano, B. Jelenkovic, C. Langer, T. Rosenband, and D. J. Wineland, Nature (London) **422**, 412 (2003).
[15] C. Piermarocchi, P. Chen, L. J. Sham, and D. G. Steel, Phys. Rev. Lett. **89**, 167402 (2002).
[16] F. Troiani, E. Molinari, and U. Hohenester, Phys. Rev. Lett. **90**, 206802 (2003).
[17] P. Chen, C. Piermarocchi, L. J. Sham, D. Gammon, and D. G. Steel, Phys. Rev. B **69**, 075320 (2004).
[18] C. J. Chang-Hasnain, P. C. Ku, J. Kim, and S. L. Chuang, Proc. IEEE **91**, 1884 (2003).
[19] W. S. Warren, H. Rabitz, and M. Dahleh, Science **259**, 1581 (1993).
[20] R. N. Zare, Science **279**, 1875 (1998).
[21] H. Rabitz, R. de Vivie-Riedle, M. Motzkus, and K. Kompa, Science **288**, 824 (2000).
[22] K. Ohmori, Y. Sato, E. E. Nikitin, and S. A. Rice, Phys. Rev. Lett. **91**, 243003 (2003).
[23] A. P. Heberle, J. J. Baumberg, and K. Kohler, Phys. Rev. Lett. **75**, 2598 (1995).
[24] X. Marie, P. LeJeune, T. Amand, M. Brousseau, J. Barrau, M. Paillard, and R. Planel, Phys. Rev. Lett. **79**, 3222 (1997).
[25] J. A. Gupta, R. Knobel, N. Samarth, and D. D. Awschalom, Science **292**, 2458 (2001).
[26] N. H. Bonadeo, J. Erland, D. Gammon, D. Park, D. S. Katzer, and D. G. Steel, Science **282**, 1473 (1998).
[27] J. Hubner, W. W. Ruhle, M. Klude, D. Hommel, R. D. R. Bhat, J. E. Sipe, and H. M. van Driel, Phys. Rev. Lett. **90**, 216601 (2003).
[28] M. J. Stevens, A. L. Smirl, R. D. R. Bhat, A. Najmaie, J. E. Sipe, and H. M. van Driel, Phys. Rev. Lett. **90**, 136603 (2003).
[29] N. H. Bonadeo, G. Chen, D. Gammon, D. S. Katzer, D. Park, and D. G. Steel, Phys. Rev. Lett. **81**, 2759 (1998).
[30] P. Borri, W. Langbein, S. Schneider, U. Woggon, R. L. Sellin, D. Ouyang, and D. Bimberg, Phys. Rev. Lett. **87**, 157401 (2001).
[31] Y. R. Shen, *The Principles of Nonlinear Optics* (John Wiley and Sons, New York, 1984).
[32] M. V. Gurudev Dutt, Jun Cheng, D. G. Steel, A. S. Bracker, D. Gammon, and L. J. Sham (unpublished).
[33] J. R. Guest, T. H. Stievater, X. Li, J. Cheng, D. G. Steel, D. Gammon, D. S. Katzer, D. Park, C. Ell, A. Thranhardt, G. Khitrova, and H. M. Gibbs, Phys. Rev. B **65**, 241310(R) ((2002).
[34] A. M. Weiner, D. E. Leaird, G. P. Wiederrecht, and K. A. Nelson, Science **247**, 1317–1319 (1990).
[35] E. Hertz, O. Faucher, B. Lavorel, F. Dalla Via, and R. Chaux, Phys. Rev. A **61**, 033816 (2000).
[36] M. F. DeCamp, D. A. Reis, P. H. Bucksbaum, and R. Merlin, Phys. Rev. B **64**, 092301 (2001).
[37] J. M. Bao, A. V. Bragas, J. K. Furdyna, and R. Merlin, Nat. Mater. **2**, 175 (2003).
[38] S. E. Economou, R. B. Liu, L. J. Sham, and D. G. Steel, Phys. Rev. B **71**, 195327 (2005).
[39] J. G. Tischler, A. S. Bracker, D. Gammon, and D. Park, Phys. Rev. B **66**, 081310(R) (2002).
[40] N. F. Scherer, A. J. Ruggerio, M. Du, and G. R. Fleming, J. Chem. Phys. **93**, 856 (1990).
[41] M. M. Wefers, H. Kawashima, and K. A. Nelson, J. Chem. Phys. **102**, 9133 (1995).
[42] V. Blanchet, C. Nicole, M. A. Bouchene, and B. Girard, Phys. Rev. Lett. **78**, 2716–2719 (1997).
[43] I. L. Chuang, N. Gershenfeld, M. Kubinec, and D. W. Leung, Proc. R. Soc. London **454**, 447 (1998).
[44] I. L. Chuang, N. Gershenfeld, and M. Kubinec, Phys. Rev. Lett. **80**, 3408 (1998).
[45] A. Shabaev, A. L. Efros, D. Gammon, and I. A. Merkulov, Phys. Rev. B **68**, 201305(R) (2003).
[46] M. Phillips and H. Wang, Phys. Rev. Lett. **89**, 186401 (2002).
[47] M. Phillips, H. Wang, I. Rumyantsev, N. H. Kwong, R. Takayama, and R. Binder, Phys. Rev. Lett. **91**, 183602 (2003).
[48] J. Tribollet, F. Bernardot, M. Menant, G. Karczewski, C. Testelin, and M. Chamarro, Phys. Rev. B **68**, 235316 (2003).
[49] T. A. Kennedy, A. Shabaev, M. Scheibner, Al. L. Efros, A. S. Bracker, and D. Gammon, Phys. Rev. B **73**, 045307 (2006).